processes

MDPI

Article

Topology Optimization Combined with a Parametric Algorithm for Industrial Synchronous Reluctance Motor Design

Tae-Hee Lee [1], Dong-Kuk Lim [1], Ki-Young Moon [2] and Kyung-Won Jeon [3,*]

[1] Department of Electrical, Electronic and Computer Engineering, University of Ulsan, Ulsan 44610, Korea; lth7486@gmail.com (T.-H.L.); ldk8745@ulsan.ac.kr (D.-K.L.)
[2] R&D Division, KSEP Co., Miryang-si 50465, Korea; kymoon@ksp-tube.co.kr
[3] Daewoo Shipbuilding & Marine Engineering Co., Geoje-si 53302, Korea
* Correspondence: jeonkw@dsme.co.kr; Tel.: +82-55-735-7145

Abstract: In this paper, we propose combining topology optimization with a parametric algorithm (TOCPA) to design an industrial synchronous reluctance motor (SynRM) that satisfies super-premium efficiency (IE4). TOCPA consists of two main processes. An improved niching algorithm is proposed as an existing parametric algorithm, and multiple optimal points were identified quickly and effectively within the design range specified by the user. Existing parametric algorithms lack the ability to find unpredictable new optimal shapes; therefore, topology optimization has been added. TOCPA converges the two optimization methods to compensate for the shortcomings of each and maximizes the advantages. In addition, the boundary surface ON–OFF method is applied to accelerate the topology optimization process. Subsequent ratio-based smoothing techniques smooth out discontinuous interfaces and remove clusters to improve the torque characteristics and reduce the manufacturing difficulty. Finally, the torque ripple was reduced using the skew technique, and mechanical stability was confirmed using a stress analysis. An IE4 industrial SynRM was successfully designed using TOCPA.

Keywords: niching algorithm; ON–OFF method; smoothing method; synchronous reluctance motor; topology optimization

Citation: Lee, T.-H.; Lim, D.-K.; Moon, K.-Y.; Jeon, K.-W. Topology Optimization Combined with a Parametric Algorithm for Industrial Synchronous Reluctance Motor Design. *Processes* **2022**, *10*, 746. https://doi.org/10.3390/pr10040746

Academic Editors: Alon Kuperman and Alessandro Lampasi

Received: 23 March 2022
Accepted: 7 April 2022
Published: 12 April 2022

1. Introduction

An interior permanent magnet synchronous motor (IPMSM) is a high-performance motor that is used in many applications. However, the rare earth permanent magnets used by an IPMSM cause environmental pollution in the processes of mining and manufacturing; therefore, they are difficult to produce. Most of the production is monopolized by specific countries. Additionally, the magnets are expensive and the supply is not stable [1]. As a result, it is necessary to study a motor that does not use a rare earth magnet.

Induction motors (IMs) are reliable, have a simple structure, and are inexpensive because rare earth magnets are not used [2–4]. In addition, IMs have the advantage of being easy to control. For this reason, approximately 70% of all industrial load on a utility is represented by IMs [5,6]. However, because IMs have been used for a long time, the development has reached saturation and it is difficult to further improve the efficiency. Therefore, it is difficult for the IMs to respond to harsh environmental regulations.

A synchronous reluctance motor (SynRM) is driven by reluctance torque using the barrier structure inside the rotor iron core. A SynRM is inexpensive because it does not use rare earth permanent magnets. In addition, because there is no squirrel-shaped copper conductor inside, it is less expensive and copper loss does not occur. Therefore, a SynRM is more advantageous than an IM, in terms of efficiency and cooling [7–10].

When determining the performance of a motor, such as SynRM, the average torque, torque ripple, and efficiency are important. These characteristics change non-linearly, according to the shape, because of the magnetic flux saturation. Therefore, the finite

element method (FEM) is used in the process of calculating the characteristic of electronic devices. The FEM is a technique that divides the analysis domain into small units and adds up each physical quantity to obtain the result. The FEM is widely used in design because it is similar to an actual experiment; however, it takes a lot of computation time. Therefore, an optimization process is needed to find the optimal design shape, while minimizing the FEM analysis [11–14].

Existing parametric algorithms can designate a range of design variables and efficiently search for an optimal shape within them. However, the parametric algorithm has limited changes in shape and has disadvantages, in that it cannot search for complex shapes compared to the initial model. Figure 1 shows the magnetic flux flow when there is only a steel core without blocks, such as a magnet or air in the rotor. To increase the salient pole ratio, it is necessary to suppress the magnetic flux flow in the other axis, without disturbing the magnetic flux flow [15–18]. Therefore, air barriers, similar to magnetic flux lines, are inserted, as shown in Figure 2. In contrast to an IPMSM, because a SynRM does not have a magnet inside the rotor, the straight-line structure is not forced, but, rather, a curved air barrier can maximize the d–q axis reluctance difference. Topology optimization (TO) is a technique suitable for finding shapes that include curves with multiple curvatures, such as the SynRM design. Because the TO directly deforms the shape and searches for the optimal shape, it is possible to search for a shape beneficial to the magnetic flux flow that the user has not predicted [19–22]. In addition, in the TO, the number of models to be explored increases exponentially, according to the material of the design target. Because the SynRM rotor has only two materials, iron and air, it is appropriate for TO. Therefore, there are many papers applying TO to SynRM [23–26].

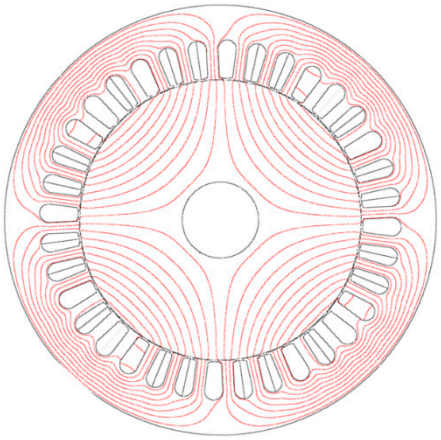

Figure 1. Magnetic flux flowing through the core.

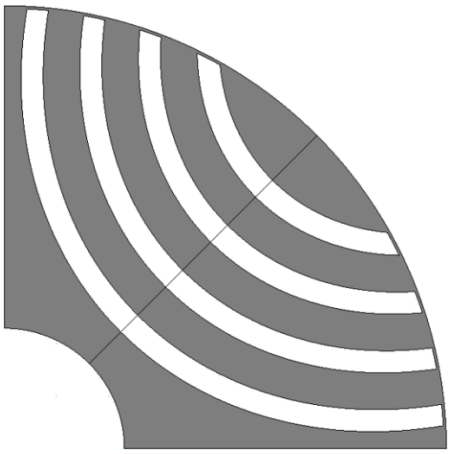

Figure 2. 90° periodic model of the SynRM rotor.

Despite the optimization of SynRM, which consists of two materials, many analyses are required to determine the optimal design with high performance. For efficient searching, the mesh grid and initial shape should be specified. A parametric algorithm, the niching algorithm (NA), was used to select the initial shape, while setting the major and minor axes of the ellipses constituting the mesh grid. Afterwards, the ON–OFF method was applied to the optimized mesh grid and the initial model. The ON–OFF method can find the optimal shape by repeatedly making models in which the cells constituting the mesh are changed one by one, determining the material by comparing the values of each objective function, and obtaining the next shape. To minimize the number of analyses required for the ON–OFF method, the ON–OFF method sequence was performed on the material boundary surface of the model only.

This paper provides a detailed description of how topology optimization is used in combination with a parametric algorithm (TOCPA), applied to an elliptical grid for high-efficiency industrial SynRM designs. The proposed optimization method yielded a model with a small torque ripple, while satisfying the required average torque, and applied post-processing techniques, such as smoothing, to design an industrial SynRM designed through optimization. The final model achieved the super-premium efficiency (IE4) requirements, with an average torque of 87.01 Nm, a torque ripple of 6.65%, a loss of 468.43 W, efficiency of 97.22%, and a safety factor of 2.67.

2. Analyzed Synchronous Reluctance Motor

The salient pole ratio, which is the ratio of the d–q axis reluctance of the SynRM design, can be expressed by Equation (1).

$$\xi = \frac{L_{ds}}{L_{qs}} \tag{1}$$

where L_{ds} is the d-axis inductance and L_{qs} is the q-axis inductance. Additionally, the torque equation of SynRM can be expressed as:

$$T = \frac{3}{2}\frac{P}{2}(L_{ds} - L_{qs})i_{ds}i_{qs} \tag{2}$$

$$T = \frac{3}{2}\frac{P}{2}(\xi - 1)\frac{{E_m}^2 \sin 2\theta}{\omega L_{ds}} \tag{3}$$

where i_{ds} and i_{qs} are the d-axis and q-axis currents, respectively, E_m is the electromotive force, θ is the power angle, and ω is the angular velocity. If ξ is sufficiently larger than one, the torque of SynRM is proportional to ξ.

Figure 2 shows the shape of the SynRM rotor to which the optimization was applied. To maximize the salient pole ratio, which is the difference in reluctance between the d-axis and q-axis, there is no structure to block the magnetic flux in the d-axis direction; however, there is a magnetic flux barrier made of air in the q-axis direction. The target motor was adopted a transversally laminated anisotropic (TLA) rotor to prevent eddy currents. The TLA rotor has a structure in which several thin steel plates of the same shape are stacked. In the TLA-type rotor, a bridge exists to mechanically connect the structure, and magnetic flux leakage occurs. However, because only one design model is required, it is easy to design and assemble; therefore, it is widely adopted [27,28].

3. Optimization Process

The target motor is a 15 kW industrial SynRM, with a stacking length of 205 mm and a stator diameter of 260 mm. The design goals are listed in Table 1 and the motor specifications are listed in Table 2. The efficiency standard of the IE4 class 15 Kw class four-pole motor is 93.9%, but since mechanical loss is not applied in the analysis, a target efficiency of 95% was set. Figure 3 shows the basic rotor and stator shapes of SynRM, and the winding structure.

Table 1. Requirements of an objective motor.

Requirement	Value
Rated power [kW]	15
Rated torque [Nm]	79.6
Torque ripple [%]	10
Efficiency [%]	95
Rated speed/Max speed [rev/min]	1800/3600
Maximum stress [MPa]	915

Table 2. Specifications of an objective motor.

Parameter	Value
Number of poles	4
Number of slots	36
Stator outer/inner diameter [mm]	260/170
Rotor outer/inner diameter [mm]	169.2/46
Air gap [mm]	0.8
Stacking length [mm]	205
Material of core	50JN290

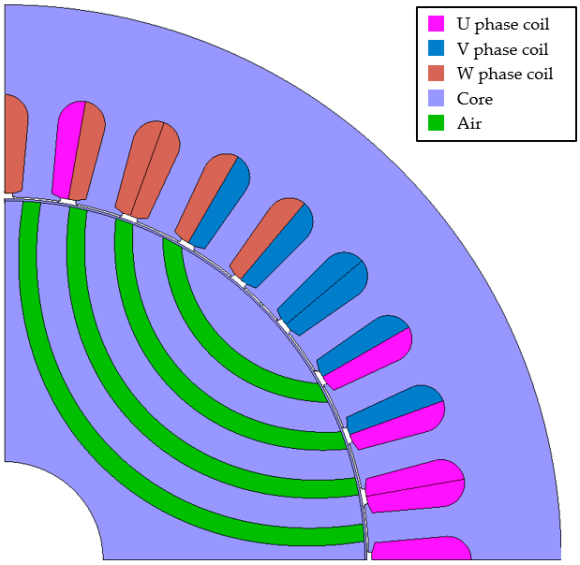

Figure 3. Basic form of SynRM to which optimization is applied.

3.1. Oval Mesh Grid

To apply TO, a mesh grid is needed to draw boundaries to divide the cells. To maximize the salient pole ratio of SynRM, as shown in Figure 2, an air barrier, in the form of using concentric circles with an outside center, is widely used. However, the magnetic flux lines shown in Figure 1 are not perfectly circular. A rotor with an elliptical structure may have higher performance. Therefore, an algorithm was applied to the SynRM sample with four air barriers to determine the optimal mesh grid. Figure 4 is a 45° sector shape design area that is a symmetrical model of a 90° periodic model of a SynRM rotor. The lengths of the elliptical radius on the x-axis and y-axis were designated as variables, and a model with four air barriers was created. The average torque, which is an objective function, was compared and optimized. Figure 5 shows the overall flow diagram of the TOCPA. Directional auto-tuning NA maintains the multi-modal search capability of the niche algorithm and compensates the problem of missing local optimal solutions because of the existing directional niche range.

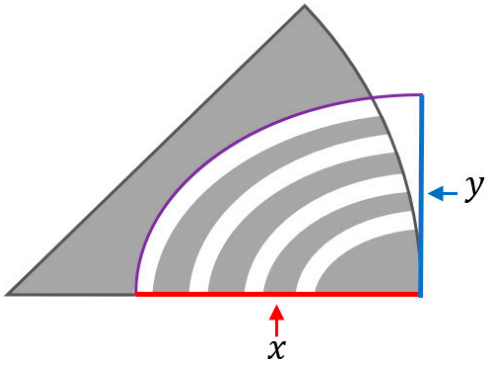

Figure 4. Design variables for SynRM optimization.

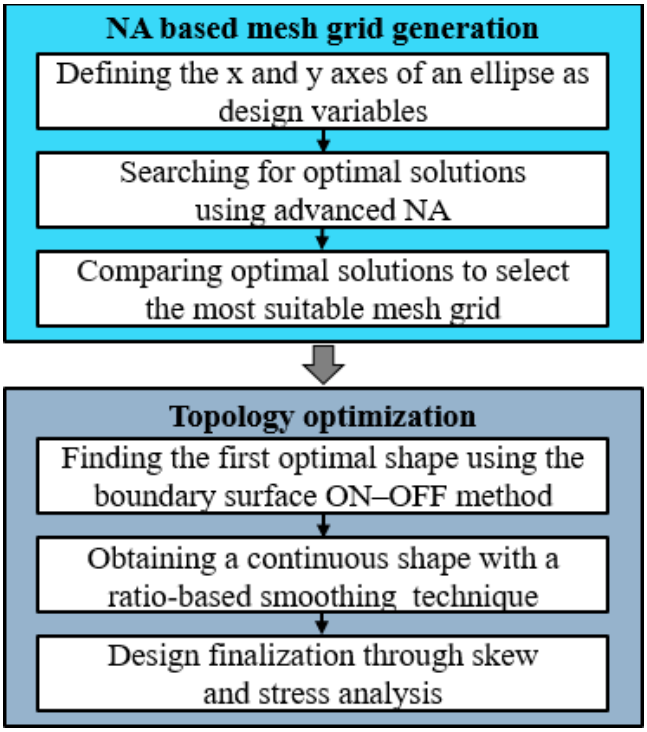

Figure 5. Flow diagram of the TOCPA.

The process of directional auto-tuning NA is as follows.

Step 1: Creation of an initial point

An initial model is created using Latin hypercube sampling (LHS) within the design range. LHS divides the sample region into a grid and sets it so that only one sample is generated in the same row and column, such that samples are generated evenly and the variable space can be searched efficiently. Figure 6 shows an example of LHS sample generation.

Step 2: Gradient descent

The gradient descent method is applied to a given model to search for an optimal point. This method finds the direction in which the slope of the objective function is steepest. If the optimum point is passed after moving, the moving interval is reduced and the search is repeated in the same way. If the movement interval is specified by the user, the maximum gradient method is terminated. The green circle in Figure 7 shows the process of finding the maximum slope. If the search point enters the niche range during the gradient descent method, it goes through the niche judgment process, and if it is regarded as a duplicate search, the process moves to Step 5.

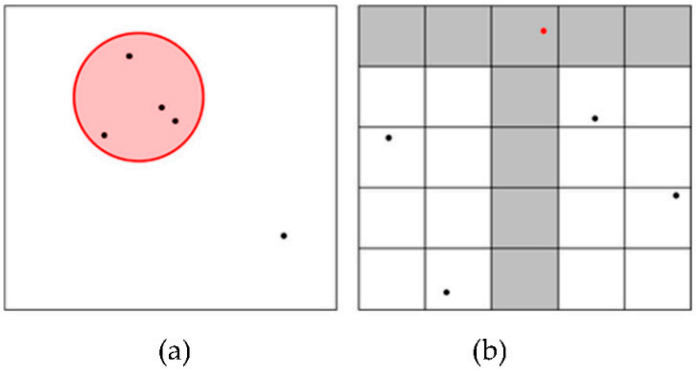

Figure 6. Conceptual diagram: (**a**) conventional sampling; (**b**) LHS.

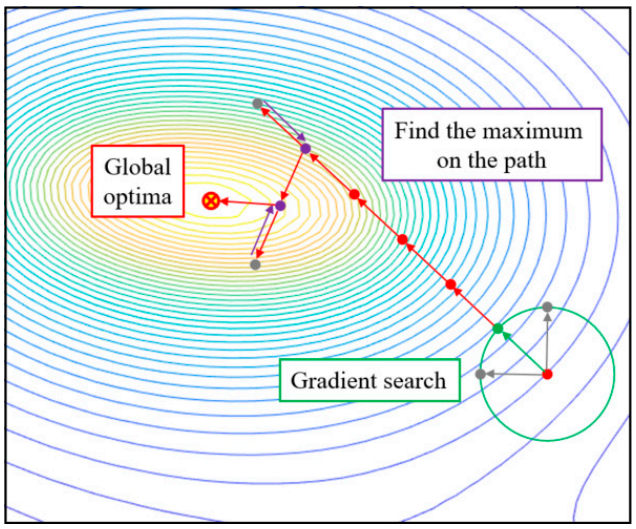

Figure 7. Conceptual diagram of the gradient descent.

Step 3: Confirmation of convergence

In the case where the maximum gradient method is terminated and the niche range is repeated *N* times, it is concluded that all the optimal points have been searched and NA is terminated.

Step 4: Directional niche region

The existing niching algorithm sometimes misses the local optimum, due to the niche range, as shown in Figure 8a. The omission of local optimal points can be dramatically reduced through the directional niche region.

As shown in Figure 8b, a sector is created with the radius of the line from the beginning of the search to the optimal point. The more the angle differs from the line, the lower the probability of determining the niche range [12].

Step 5: Confirmation of the niche range

If a point is generated within the directional niche range, the probability specified in Step 4 is applied to judge whether it is a duplicate, and if it is a duplicate, the process goes to Step 4. If the duplicate check is passed, the process goes to Step 2.

As a result of applying NA, four optimal design points were found. The shape and magnetic flux density of each model were confirmed in Figure 9, and the torque and torque ripple were confirmed in Table 3. Model a, which is the model with the smallest torque ripple among the models that achieved the required output, was selected and then applied to the optimization process.

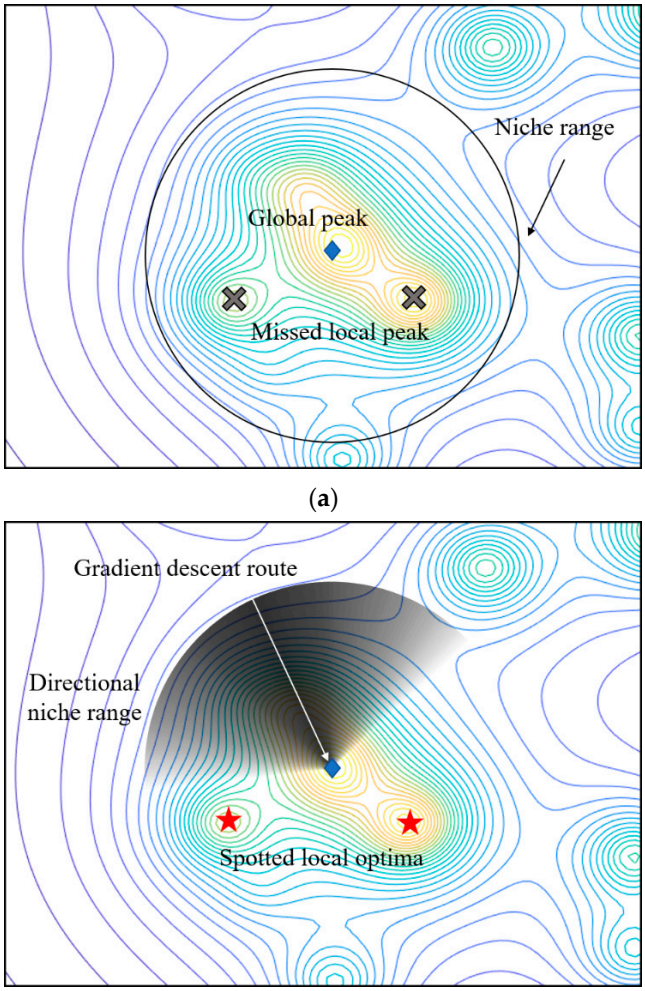

Figure 8. Conceptual diagram: (**a**) existing NA; (**b**) proposed NA.

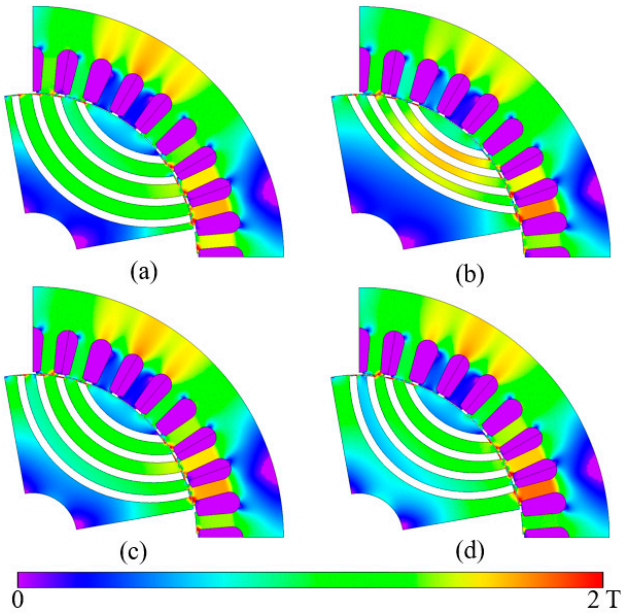

Figure 9. Shape and magnetic flux density of the SynRM models with directional auto-tuning NA applied. (**a**) model a, (**b**) model b, (**c**) model c, (**d**) model d.

Table 3. Average torque and torque ripple of 4 models as a result of NA optimization.

Model	T_{ave} (Nm)	T_{ripple} (%)
a	90.04	18.64
b	85.79	24.34
c	89.54	22.99
d	87.76	18.45

3.2. ON–OFF Method

The ON–OFF method uses a mesh grid that divides the designed target area into small pieces, to determine which material will be assigned to each cell. An example of a mesh grid is shown in Figure 10. The material of the cell is designated by comparing the objective function value of the existing model and model in which one cell has been changed. Therefore, the number of analyses is the number of cells, and if the number of materials increases, the number of required analyses increases exponentially. The number of analyses required to proceed with one step of the ON–OFF method can be expressed as $N_c^{N_m}$, where N_c is the number of cells and N_m is the number of types of material. In the case of SynRM, it is advantageous to apply the ON–OFF method because there are only two materials, air and iron. The ON–OFF method consists of the following processes:

(*Processes 1*) The initial model and mesh grid are set.
(*Processes 2*) The objective function value of the initial model is calculated through FEM.
(*Processes 3*) The objective function value of the model in which one cell is changed from the initial model is obtained. This repeats *i* from one to the last cell number.
(*Processes 4*) If the objective function value of model *i* is better than the existing value, the material of cell *i* is changed.
(*Processes 5*) At this time, to prevent over convergence, the material change factor P, which is a value between zero and one, is used, and the cells corresponding to 1-*P* of the entire lower level are not changed.
(*Processes 6*) Processes 2–4 are repeated until there are no more changed cells.

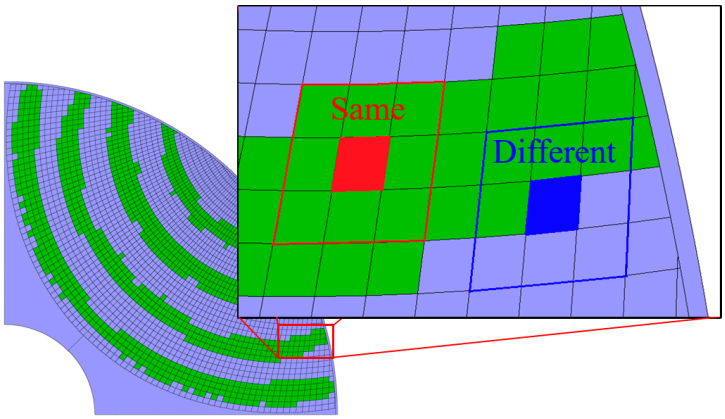

Figure 10. An example of cells excluded from analysis.

By setting the design result of the parametric algorithm as the initial model, the ON–OFF method can proceed quickly. If the initial model is not applied, the ON–OFF method does not cause meaningful change in the FEM analysis result, does not converge, or takes a long time.

Additionally, if the mesh grid is not dense enough, the set size of the cell is large. In this state, when the material of the cell is changed, a large area is inverted to produce a shape that protrudes more than necessary, which causes a problem that leads to good characteristics being difficult to determine compared with the initial shape.

However, as the number of cells increases, the number of analyses required for the ON–OFF process increases and more time is required. To solve this problem, if nine cells,

including the target cell, are of the same material as the red cell in Figure 10, the target cell becomes an excluded cell and the ON–OFF analysis is not performed. Conversely, if even one of the nine cells is made of a different material, it becomes an interpreted cell and the ON–OFF analysis proceeds. This boundary-surface ON–OFF method can also minimize the cluster generation in the existing ON–OFF process.

The ON–OFF method changed the layers and identified a model with an average torque of 90.02 Nm and a torque ripple of 28.11%. The model obtained through the ON–OFF method is shown in Figure 11. The average torque increased; however, the torque ripple also increased. Therefore, additional techniques are needed to reduce torque ripple.

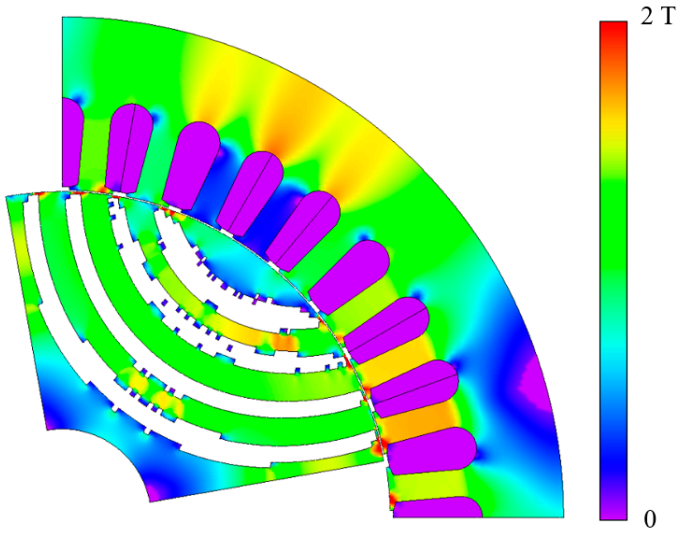

Figure 11. Shape and magnetic flux density of the SynRM model with the ON–OFF method.

3.3. Smoothing

The shape obtained by the ON–OFF method has a discontinuous interface, which disturbs the smooth flux flow and increases the manufacturing difficulty. Therefore, a smoothing technique should be applied to change the uneven interface into a smooth curved shape. The smoothing technique draws a curve by determining the ratio through the number of horizontal lines that intersect along the boundary at the point where the surface is discontinuous. The boundary is determined so that the area of the converted material is similar; this process is shown in Figure 12.

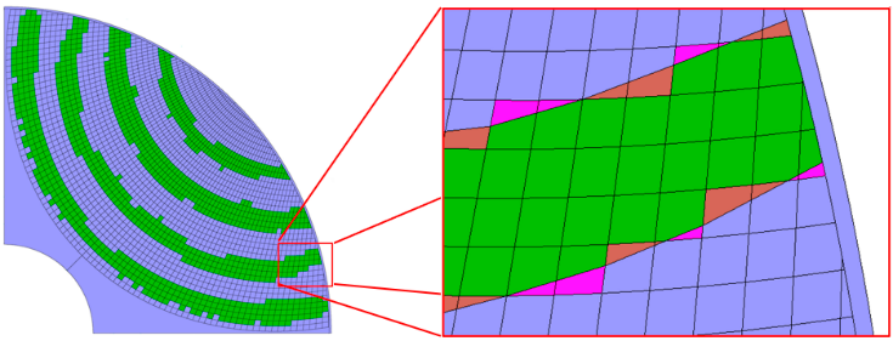

Figure 12. An example of the smoothing technique.

The shape obtained through the smoothing technique has an average torque of 91.24 Nm and a torque ripple of 11.21%, which is better than the 90.02 Nm and 28.11% of the ON–OFF optimization model. The manufacturing difficulty was also reduced, as shown in Figure 13.

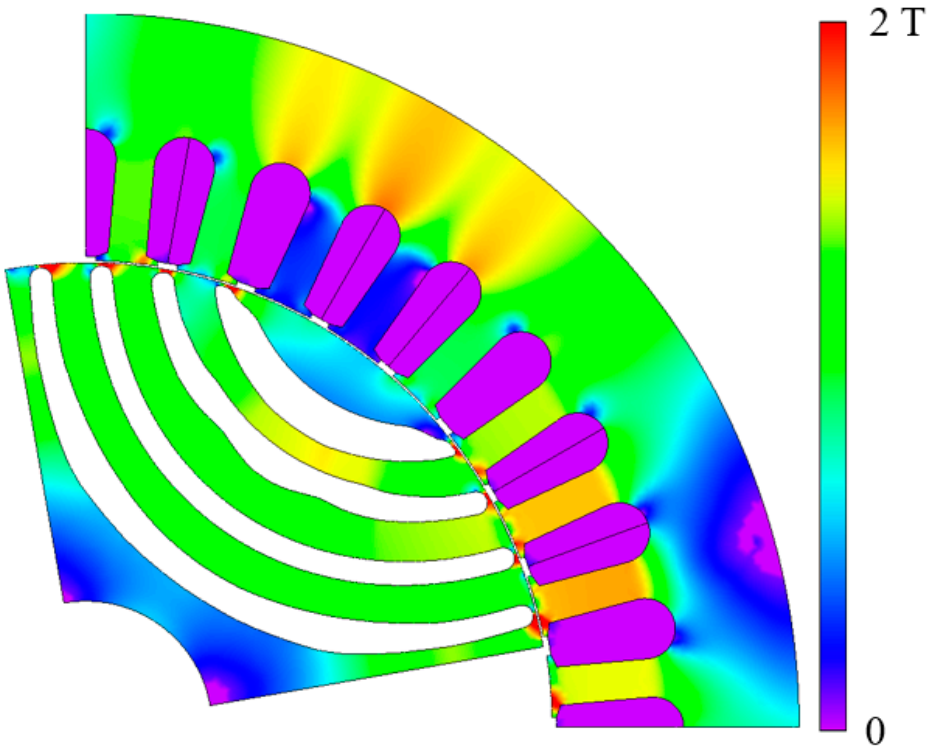

Figure 13. Shape and magnetic flux density of the SynRM model with the smoothing technique.

3.4. Skew

By using the TO, the torque was greater than that of the model obtained by parameter optimization. However, the torque ripple also increased. As a result, the skew technique was used to reduce the torque ripple. The skew technique was applied by dividing the rotor in the axial direction, as shown in Figure 14, and twisting it as much as the skew angle. As the torque waveform of each part is distorted, there is a slight loss in the average torque; however, the effect of greatly offsetting the torque ripple can be obtained. The torque waveform is shown in Figure 15 and details are listed in Table 4.

Table 4. Average torque and torque ripple changes according to the topology optimization steps.

Model	T_{ave} (Nm)	T_{ripple} (%)
Initial	80.22	48.10
NA	87.76	18.45
ON–OFF	90.02	28.11
Smoothing	91.24	11.21
Skew	87.01	6.65

3.5. Stress Analysis

Although SynRM is mechanically more stable than permanent magnet devices, the rotor can be broken by centrifugal force at high speed. It is, therefore, necessary to verify the mechanical stability through a stress analysis.

The results of the stress analysis at the speed of 3600 RPM (maximum speed) show that the maximum stress of the optimized model was 343 MPa. Therefore, the safety factor is 2.67, which ensures sufficient mechanical stability. Figure 16 shows the results of the stress analysis, where the point of maximum stress in the bridge is shown in red.

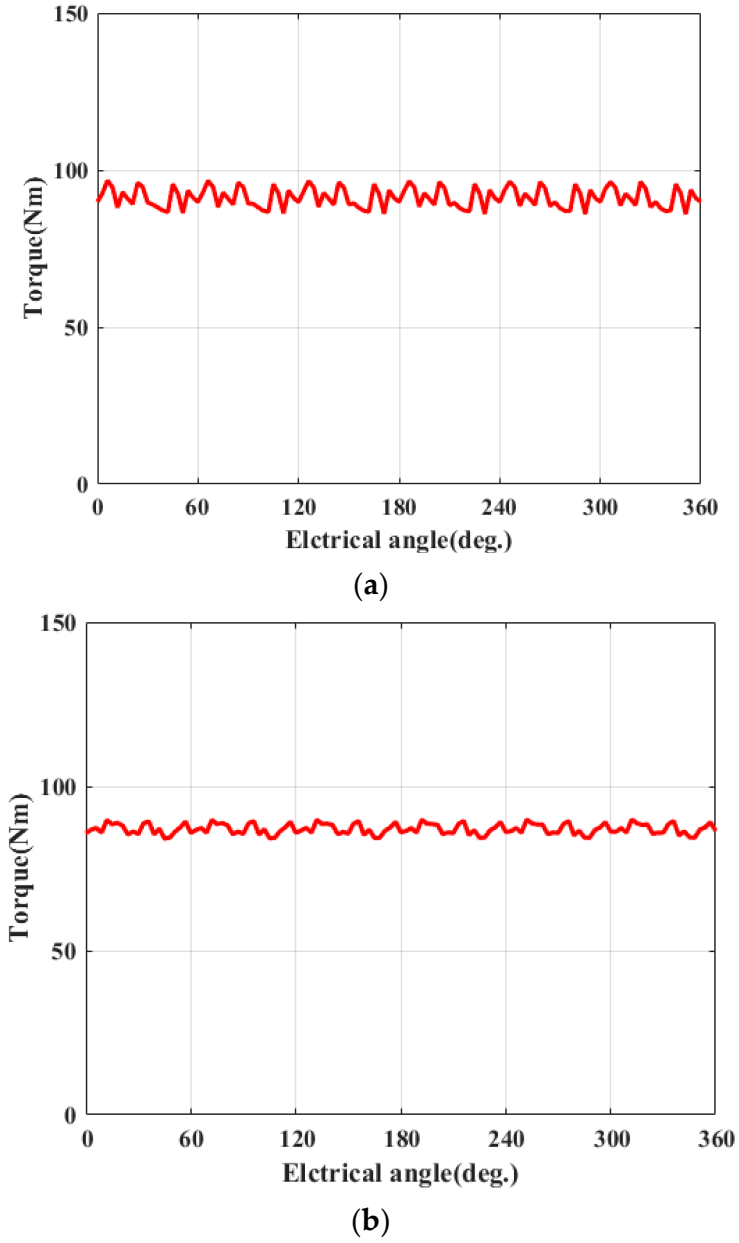

Figure 14. Torque waveform of the model: (**a**) non-skewed model; (**b**) skewed model.

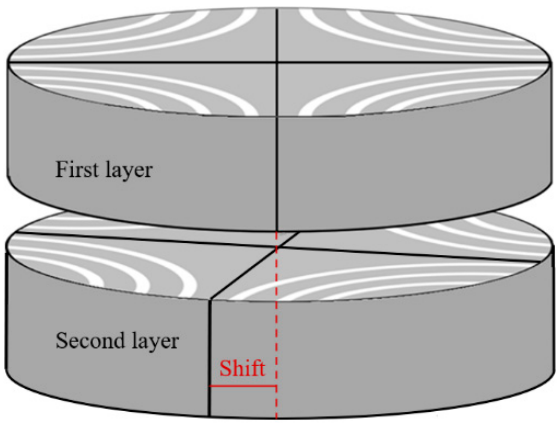

Figure 15. Instructions for applying the skew technique.

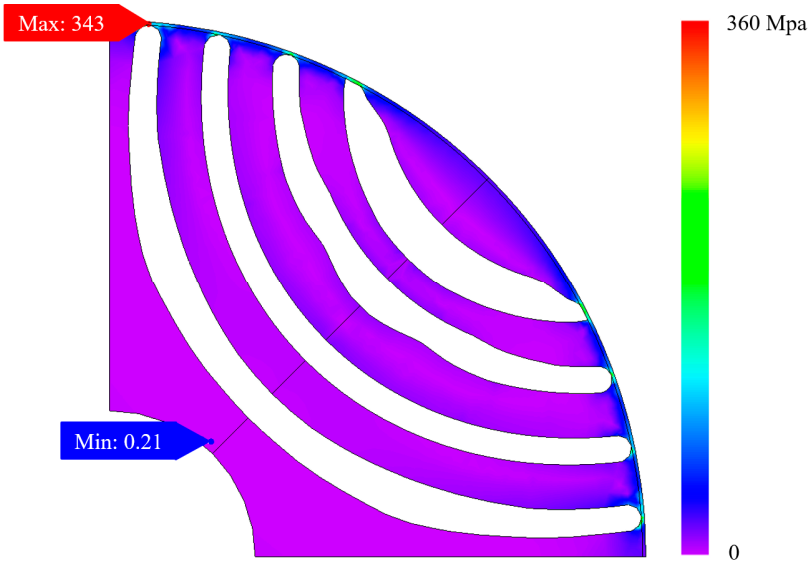

Figure 16. Results of the stress analysis.

4. Conclusions

In this paper, we successfully designed a high-performance rotor by applying TOCPA to the industrial IE4 SynRM optimal design problem. In the proposed TOCPA, the optimal shape was searched more efficiently by optimizing the elliptical mesh grid as a parametric algorithm and applying the ON–OFF method to the boundary surface only. The initially set design goals were achieved with an average torque of 87.01 Nm, a torque ripple of 6.65%, a loss of 468.43 W, an efficiency of 97.22%, and a safety factor of 2.67. The TOCPA can be used to find a design that is advantageous for magnetic flux characteristics with an unexpected structure. In the final model, slight unevenness further reduced the torque ripple.

The advantages of the proposed TOCPA are summarized as follows:

- The optimization process for the initial design, mesh grid setting, and boundary surface ON–OFF method are the most efficient ways to use TO.
- The TOCPA applied determines an optimal design that breaks stereotypes. This cannot be achieved with conventional optimization methods using a limited number of design variables.
- Finally, a ratio-based smoothing technique was applied that can reduce the manufacturing difficulty and obtain additional performance improvements.

For these reasons, this research is noteworthy, in that the proposed TOCPA can be widely used in a variety of electrical machine designs using FEM. In addition, in order to further improve TOCPA, we are developing an automation code that binds cells of the same material to one region when analyzing them. During the analysis process, it takes a long time to give conditions to each region. This automation code will drastically reduce the time spent on conditioning.

Author Contributions: Investigation, T.-H.L.; writing—original draft preparation, T.-H.L.; writing—review and editing, D.-K.L., K.-Y.M. and K.-W.J. All authors have read and agreed to the published version of the manuscript.

Funding: This research received no external funding.

Institutional Review Board Statement: Not applicable.

Informed Consent Statement: Not applicable.

Data Availability Statement: Not applicable.

Acknowledgments: This research was supported by "Regional Innovation Strategy (RIS) through the National Research Foundation of Korea (NRF) funded by the Ministry of Education (MOE) (2021RIS-003)".

Conflicts of Interest: The authors declare no conflict of interest.

References

1. Zou, G.; Cai, S. Research on Chinese rare earth industry government regulation based on SCP theory paradigm. In Proceedings of the International Conference on Remote Sensing 2011, Environment and Transportation Engineering, Nanjing, China, 24–26 June 2011; Volume 27.
2. De Martin, M.; Luise, F.; Pieri, S.; Tessarolo, A.; Poloni, C. Numerical multi-objective optimization of a squirrel cage induction motor for industrial application. In Proceedings of the 2015 International Aegean Conference on Electrical Machines & Power Electronics (ACEMP), Side, Turkey, 2–4 September 2015.
3. Li, H.; Curiac, R.S. Designing More Efficient Large Industrial Induction Motors by Utilizing the Advantages of Adjustable-Speed Drives. *IEEE Trans. Ind. Appl.* **2010**, *46*, 1805–1809. [CrossRef]
4. Staton, D.; Boglietti, A.; Cavagnino, A. Solving the More Difficult Aspects of Electric Motor Thermal Analysis in Small and Medium Size Industrial Induction Motors. *IEEE Trans. Energy Convers.* **2005**, *20*, 3. [CrossRef]
5. Maljkovic, Z.; Cettolo, M.; Pavlica, M. The Impact of the Induction Motor on Short-Circuit Current. *IEEE Ind. Appl. Mag.* **2001**, *7*, 11–17. [CrossRef]
6. Waide, P.; Brunner, C.U. *Energy-Efficiency Policy Opportunities for Electric Motor-Drive Systems*; International Energy Agency: Paris, France, 2011.
7. Jeong, S.-W. Optimal Design of IE4 Super Premium Efficiency Synchronous Reluctance Motor for Industrial Applicatio. Master's Thesis, Department Electrical and Information Engineering, Seoul University, Seoul, Korea, 2020.
8. Park, J.H.; Seo, J.H.; Cha, C.H.; Lee, J. Characteristics Analysis of 15kW Industrial Machine using Synchronous Reluctance Motor for High Efficiency. In Proceedings of the 2013 International Conference on Electrical Machines and Systems (ICEMS), Busan, Korea, 26–29 October 2013.
9. Weigel, T. Control of Synchronous Reluctance Motors without Encoder for Industrial Applications. In Proceedings of the 2016 6th International Electric Drives Production Conference, Nuremberg, Germany, 30 November–1 December 2016.
10. Miller, T.J.E.; Hutton, A.; Cossar, C.; Staton, D.A. Design of a Synchronous Reluctance Motor Drive. *IEEE Trans. Ind. Appl.* **1991**, *27*, 741–749. [CrossRef]
11. Kang, Y.-R.; Son, J.-C.; Lim, D.-K. Optimal Design of IPMSM for Fuel Cell Electric Vehicles Using Autotuning Elliptical Niching Genetic Algorithm. *IEEE Access* **2020**, *8*, 117405–117412. [CrossRef]
12. Lee, T.H.; Kang, Y.R.; Son, J.C.; Lim, D.K. Optimized Design of Permanent Magnet Assisted Synchronous Reluctance Motor Using Oriented Auto-tuning Niching Algorithm. *J. Electr. Eng. Technol.* **2021**, *16*, 1495–1503. [CrossRef]
13. Son, J.-C.; Ahn, J.-M.; Lim, J.-W.; Lim, D.-K. Optimal Design of PMa-SynRM for Electric Vehicles Exploiting Adaptive-Sampling Kriging Algorithm. *IEEE Access* **2021**, *9*, 41174–41183. [CrossRef]
14. Liu, X.; Fu, W.N. A Dynamic Dual-Response-Surface Methodology for Optimal Design of a Permanent-Magnet Motor Using Finite-Element Method. *IEEE Trans. Magn.* **2016**, *52*, 7204304. [CrossRef]
15. Mohanarajah, T.; Rizk, J.; Nagrial, M.; Hellany, A. Design Optimisation of Flux Barrier Synchronous Reluctance Machines. In Proceedings of the 2015 Intl Aegean Conference on Electrical Machines & Power Electronics (ACEMP), 2015 Intl Conference on Optimization of Electrical & Electronic Equipment (OPTIM) & 2015 Intl Symposium on Advanced Electromechanical Motion Systems (ELECTROMOTION), Side, Turkey, 2–4 September 2015.
16. Ding, H.; Zhu, H.; Hua, Y. Optimization Design of Bearingless Synchronous Reluctance Motor. *IEEE Trans. Appl. Supercond.* **2018**, *28*, 5202905. [CrossRef]
17. Liu, C.; Wang, K.; Wang, S.; Wang, Y.; Zhu, J. Torque Ripple Reduction of Synchronous Reluctance Machine by Using Asymmetrical Barriers and Hybrid Magnetic Core. *CES Trans. Electr. Mach. Syst.* **2021**, *5*, 13–20. [CrossRef]
18. Pellegrino, G.; Cupertino, F.; Gerada, C. Automatic Design of Synchronous Reluctance Motors Focusing on Barrier Shape Optimization. *IEEE Trans. Ind. Appl.* **2015**, *51*, 1465–1474. [CrossRef]
19. Takahashi, N.; Nakazaki, S.; Miyagi, D. Examination of Optimal Design Method of Electromagnetic Shield Using ON/OFF Method. *IEEE Trans. Magn.* **2009**, *45*, 1546–1549. [CrossRef]
20. Zhao, F.; Yan, R. Topology Optimization of Magnetic Actuator Using the Improved ON/OFF Method. In Proceedings of the 2012 Sixth International Conference on Electromagnetic Field Problems and Applications, Dalian, China, 19–21 June 2012.
21. Okamoto, Y.; Tominaga, Y.; Sato, S. Topological Design for 3-D Optimization Using the Combination of Multistep Genetic Algorithm with Design Space Reduction and Nonconforming Mesh Connection. *IEEE Trans. Magn.* **2012**, *48*, 515–518. [CrossRef]
22. Choi, N.S.; Kim, D.H.; Lee, H.B.; Byun, J.K. Topology Optimization of Dielectric Resonator in 3-D Waveguide Structure Considering Higher Mode Incidence. *IEEE Trans. Magn.* **2012**, *48*, 559–562. [CrossRef]
23. Lee, T.H.; Lee, J.H.; Yi, K.P.; Lim, D.K. Optimal Design of a Synchronous Reluctance Motor Using a Genetic Topology Algorithm. *Processes* **2021**, *9*, 1778. [CrossRef]

24. Watanabe, K.; Suga, T.; Kitabatake, S. Topology Optimization Based on the ON/OFF Method for Synchronous Motor. *IEEE Trans. Magn.* **2018**, *54*, 7201104. [CrossRef]
25. Kim, Y.S.; Park, I.H. Topology Optimization of Rotor in Synchronous Reluctance Motor Using Level Set Method and Shape Design Sensitivity. *IEEE Trans. Appl. Supercond.* **2010**, *20*, 1093–1096.
26. Sato, S.; Sato, T.; Igarashi, H. Topology Optimization of Synchronous Reluctance Motor Using Normalized Gaussian Network. *IEEE Trans. Magn.* **2015**, *51*, 8200904. [CrossRef]
27. Vagati, A.; Canova, A.; Chiampi, M.; Pastorelli, M.; Repetto, M. Design Refinement of Synchronous Reluctance Motors Through Finite-Element Analysis. *IEEE Trans. Ind. Appl.* **2000**, *36*, 1094–1102. [CrossRef]
28. Abeyrathne, I.P.; Toulabi, M.S.; Filizadeh, S. Design Optimization and Performance Prediction of Synchronous Reluctance Motors. In Proceedings of the 21st International Conference on Electrical Machines and Systems (ICEMS), Jeju, Korea, 7–10 October 2018.